

Ferroelectric effect and equivalent polarization charge model of $PbZr_{0.2}Ti_{0.8}O_3$ on AlGaN/GaN MIS-HEMT

Yao-Peng Zhao(赵垚澎), Chong Wang(王冲), Xue-Feng Zheng(郑雪峰), Xiao-Hua Ma(马晓华), Ang Li(李昂), Kai Liu (刘凯), Yun-Long He(何云龙), Xiao-Li Lu(陆小力), Yue Hao(郝跃)

Citation: Chin. Phys. B, 2021, 30 (**5**): 057302. DOI: 10.1088/1674-1056/abd469
Journal homepage: http://cpb.iphy.ac.cn; http://iopscience.iop.org/cpb

What follows is a list of articles you may be interested in

Interface and border trapping effects in normally-off Al_2O_3/AlGaN/GaN MOS-HEMTs with different post-etch surface treatments

Si-Qi Jing(荆思淇), Xiao-Hua Ma(马晓华), Jie-Jie Zhu(祝杰杰)†, Xin-Chuang Zhang(张新创), Si-Yu Liu(刘思雨), Qing Zhu(朱青), and Yue Hao(郝跃)

Chin. Phys. B, 2020, 29 (**10**): 107302. DOI: 10.1088/1674-1056/ab99bb

Comparative study on characteristics of Si-based AlGaN/GaN recessed MIS-HEMTs with HfO_2 and Al_2O_3 gate insulators

Yao-Peng Zhao(赵垚澎), Chong Wang(王冲), Xue-Feng Zheng(郑雪峰), Xiao-Hua Ma(马晓华), Kai Liu(刘凯), Ang Li(李昂), Yun-Long He(何云龙), Yue Hao(郝跃)

Chin. Phys. B, 2020, 29 (**8**): 087304. DOI: 10.1088/1674-1056/ab8daa

Method of evaluating interface traps in Al_2O_3/AlGaN/GaN high electron mobility transistors

Si-Qin-Gao-Wa Bao(包斯琴高娃), Xiao-Hua Ma(马晓华), Wei-Wei Chen(陈伟伟), Ling Yang(杨凌), Bin Hou(侯斌), Qing Zhu(朱青), Jie-Jie Zhu(祝杰杰), Yue Hao(郝跃)

Chin. Phys. B, 2019, 28 (**6**): 067304. DOI: 10.1088/1674-1056/28/6/067304

Short-gate AlGaN/GaN high-electron mobility transistors with BGaN buffer

Tie-Cheng Han(韩铁成), Hong-Dong Zhao(赵红东), Xiao-Can Peng(彭晓灿)

Chin. Phys. B, 2019, 28 (**4**): 047302. DOI: 10.1088/1674-1056/28/4/047302

Mechanism of Ti/Al/Ni/Au ohmic contacts to AlGaN/GaN heterostructures via laser annealing

Mingchen Hou(侯明辰), Gang Xie(谢刚), Kuang Sheng(盛况)

Chin. Phys. B, 2019, 28 (**3**): 037302. DOI: 10.1088/1674-1056/28/3/037302

Ferroelectric effect and equivalent polarization charge model of $PbZr_{0.2}Ti_{0.8}O_3$ on AlGaN/GaN MIS-HEMT*

Yao-Peng Zhao(赵垚澎), Chong Wang(王冲)†, Xue-Feng Zheng(郑雪峰)‡, Xiao-Hua Ma(马晓华), Ang Li(李昂), Kai Liu (刘凯), Yun-Long He(何云龙), Xiao-Li Lu(陆小力) and Yue Hao(郝跃)

Key Laboratory of Wide Band-Gap Semiconductor Materials and Devices, School of Microelectronics, Xidian University, Xi'an 710071, *China*

(Received 11 November 2020; revised manuscript received 10 December 2020; accepted manuscript online 17 December 2020)

$PbZr_{0.2}Ti_{0.8}O_3$ (PZT) gate insulator with the thickness of 30 nm is grown by pulsed laser deposition (PLD) in AlGaN/GaN metal–insulator–semiconductor high electron mobility transistors (MIS-HEMTs). The ferroelectric effect of PZT AlGaN/GaN MIS-HEMT is demonstrated. The polarization charge in PZT varies with different gate voltages. The equivalent polarization charge model (EPCM) is proposed for calculating the polarization charge and the concentration of two-dimensional electron gas (2DEG). The threshold voltage (V_{th}) and output current density (I_{DS}) can also be obtained by the EPCM. The theoretical values are in good agreement with the experimental results and the model can provide a guide for the design of the PZT MIS-HEMT. The polarization charges of PZT can be modulated by different gate-voltage stresses and the V_{th} has a regulation range of 4.0 V. The polarization charge changes after the stress of gate voltage for several seconds. When the gate voltage is stable or changes at high frequency, the output characteristics and the current collapse of the device remain stable.

Keywords: PZT, AlGaN/GaN, MIS-HEMT, equivalent polarization charge model (EPCM)

PACS: 73.40.Kp, 73.40.Rw, 73.40.Qv, 73.61.Ey **DOI:** 10.1088/1674-1056/abd469

1. Introduction

AlGaN/GaN high electron mobility transistors (HEMTs) have a two-dimensional electron gas (2DEG) with high electron density and mobility in the channel because of the spontaneous polarization and piezoelectric polarization,[1–4] and they are well suited for applications in power switching devices.[5–8] The integration of ferroelectric materials and AlGaN/GaN has attracted much attention because of exhibiting some unusual characteristics.[9,10] Recently, some ferroelectrics have been integrated with GaN-based HEMTs, such as $PbZr_xTi_{1-x}O_3$ (PZT). The polarization of PZT is several orders of magnitude larger than that of AlGaN/GaN and is variable and reversible when different electric intensities are applied.[11] Moreover, the polarization of PZT can modulate the 2DEG density of AlGaN/GaN heterojunctions, and this has been reported in some studies.[11,12]

Gate dielectric material is of vital importance for MIS-HEMTs.[13,14] Different from the traditional oxide and nitride, ferroelectric materials have strong polarization effect, resulting in the modulation of the 2DEG density and the current density.[15] The nonlinear polarization characteristics of ferroelectric materials make it possible to modulate the 2DEG density under the gate without sacrificing the gate-control ability.[15] However, few articles have reported the specific calculation model of the PZT gate dielectric for the AlGaN/GaN MIS-HEMTs.

In this paper, AlGaN/GaN MIS-HEMTs with $Pb(Zr,Ti)O_3$ (PZT) ferroelectric gate dielectric are fabricated. The PZT gate dielectric is grown by pulsed laser deposition (PLD). A theoretical calculation model of polarization charge is proposed. Moreover, the DC and pulse characteristics are analyzed.

2. Device fabrication

The AlGaN/GaN heterojunction structure used in this paper was grown on the sapphire substrate by the metal organic chemical vapor deposition (MOCVD) method. The wafer consists of an AlN nucleation layer, an AlGaN gradient layer that the Al percent is from 8% to 0, a 1-μm-thick undoped GaN layer, a 160-nm-thick undoped GaN channel, and a 25-nm-thick undoped $Al_{0.25}Ga_{0.75}N$ barrier layer. Room temperature Hall measurements of the epi-wafer yield an electron sheet density of 9.2×10^{12} cm^{-2} and an electron mobility of 1986 $cm^2/V{\cdot}s$.

The mesa area was formed by using BCl_3/Cl_2 plasma etching in an inductively coupled plasma (ICP) system followed by the drain/source Ohmic contact formation using Ti/Al/Ni/Au (30 nm/180 nm/40 nm/60 nm) annealed at 840 °C for 30 s. A 60-nm-thick Si_3N_4 layer was deposited on the surface by the plasma enhanced chemical vapor deposition (PECVD), and the Si_3N_4 of the gate area was removed by CF_4/O_2 plasma etching. Then, the PZT dielectric layer was

*Project supported by the National Natural Science Foundation of China (Grant Nos. 61974111, 62004150, and 61974115), the China Postdoctoral Science Foundation (Grant No. 2018M643575), and the Civil Aerospace Pre-Research Plan of China (Grant No. B0202).

†Corresponding author. E-mail: chongw@xidian.edu.cn

‡Corresponding author. E-mail: xfzheng@mail.xidian.edu.cn

© 2021 Chinese Physical Society and IOP Publishing Ltd

deposited by pulsed laser deposition (PLD) with the thickness of 30 nm. Then, Ni/Au E-beam evaporation and lift off were carried out to form the gate electrode. The L_g, L_{gd}, and L_{ds} of the devices are 1.0 μm, 3.5 μm, and 7.0 μm, respectively. The W_g of the devices are 50 μm. Figure 1 shows the schematic cross-sectional structure of the gate recessed MIS-HEMT. Figure 2 shows the photomicrograph of the MIS-HEMT. The parameters of the devices were measured by Keithley 4200.

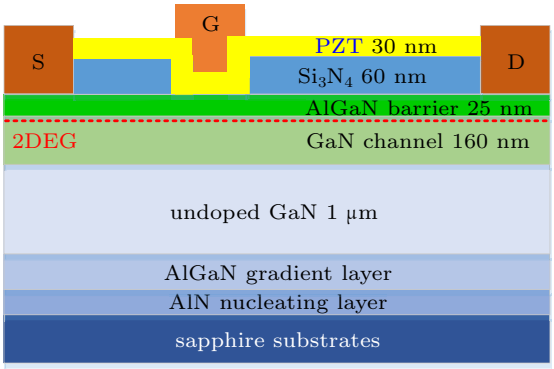


Fig. 1. The schematic cross-sectional structure of PZT AlGaN/GaN MIS-HEMT.

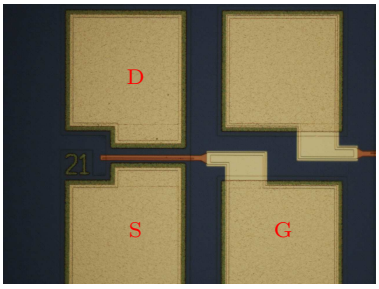


Fig. 2. The photomicrograph of the MIS-HEMT device.

3. Results and discussion

Figure 3(a) shows the transfer characteristics of the four sweeping speeds of gate voltage. The maximum drain current density reaches 800 mA/mm with the drain voltage of 10 V when the gate voltage sweeping speed is 2 V/s. The current density decreases to 450 mA/mm when the sweeping speed is up to 20 V/s. For the same device, as the change of polarization charge takes time, the amount of polarization charges in PZT is different at different sweeping speeds and different amount of polarization charge leads to different current densities. The peak trans-conductance decreases from 122 mS/mm to 40 mS/mm when the scanning speed is 2 V/s and 20 V/s, respectively. The trans-conductance decreases due to the depletion of electrons in the channel by the polarization charge. When the sweeping speed is 20 V/s, the polarization charge cannot keep pace with the change of the gate voltage, which results in the decrease of the current density. The calculation model of polarization charge will be presented in the following part.

Figure 3(b) shows the transfer curve in logarithmic coordinates. Excellent off-state performance was achieved with a low leakage current of about 10^{-10} A/mm. The threshold voltage (V_{th}) in this paper is defined as the gate bias when the drain current reaches 1 mA/mm. The V_{th} increases from −12.2 V to −8 V when the scanning speed is 2 V/s and 20 V/s, respectively. The change of polarization charge can modulate the V_{th}, and the modulation range is up to 4.2 V, which is an effective method to realize the enhancement-mode devices.

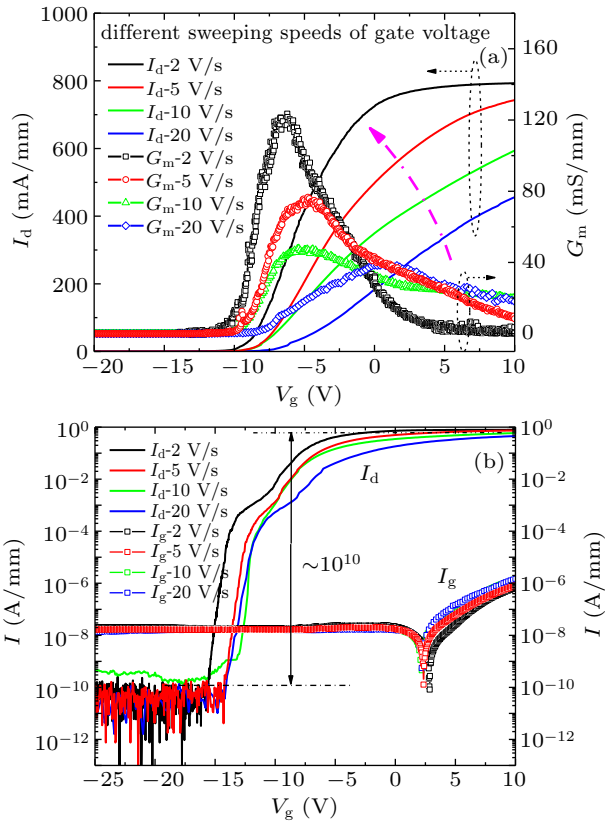


Fig. 3. Transfer characteristic curves of different sweeping speeds of gate voltage (a) conventional coordinates and (b) logarithmic coordinates.

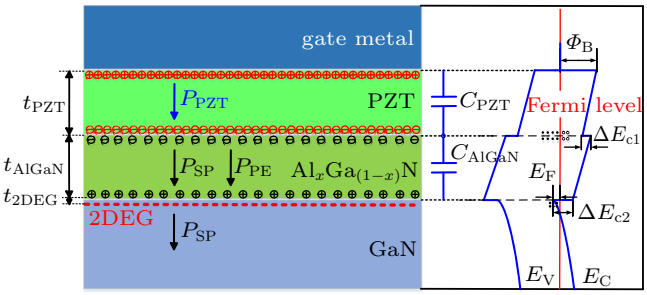


Fig. 4. Polarization charge diagram and energy band diagram of PZT MIS-HEMT.

The polarization charges and energy band of MIS-HEMT are shown in Fig. 4. In AlGaN/GaN heterojunction, electrons will be confined at the interface because of spontaneous polarization and piezoelectric polarization. To calculate the amount of the polarization-induced sheet charge density σ at the AlGaN/GaN interface, we use the following set of linear interpolations between the physical properties of GaN and AlN[16] (the x is the Al-content of the $Al_xGa_{1-x}N$ barrier):

$$\sigma(x) = |P_{PE}(\text{AlGaN}) + P_{SP}(\text{AlGaN}) - P_{SP}(\text{GaN})|$$

$$= \left| 2 \cdot \frac{a(0)-a(x)}{a(x)} \left\{ e_{31}(x) - e_{33}(x) \frac{C_{13}(x)}{C_{33}(x)} \right\} + P_{\mathrm{SP}}(x) - P_{\mathrm{SP}}(0) \right|, \quad (1)$$

where $a(x)$ is lattice constant, $C_{13}(x)$ and $C_{33}(x)$ are elastic constants, $e_{33}(x)$ and $e_{31}(x)$ are piezoelectric constants, $P_{\mathrm{sp}}(x)$ is spontaneous polarization. The specific calculation methods of these parameters are shown in Ref. [16]. When x is 0.25, $\sigma(x)$ is 0.022 C/m^2.

The distance between PZT polarization charge and 2DEG is large compared with the σ of the AlGaN/GaN interface. The force between the polarization charge and the electrons in the channel is inversely proportional to the distance. We propose an equivalent polarized charge model (EPCM) with the calculation method as given in Eq. (2), it can be used to calculate the effect of both the PZT and AlGaN polarization charges on the 2DEG. $\sigma'(x)$ is the equivalent polarization charge.

$$\sigma'(x) = \sigma(x) \cdot (1 + k \cdot \frac{P_{\mathrm{PZT}}}{\sigma(x)}) = \sigma(x) \cdot \left(1 + \frac{\frac{P_{\mathrm{PZT}}}{t_{2\mathrm{DEG}} + t_{\mathrm{AlGaN}}} + \frac{-P_{\mathrm{PZT}}}{t_{2\mathrm{DEG}} + t_{\mathrm{AlGaN}} + t_{\mathrm{PZT}}}}{\frac{\sigma(x)}{t_{2\mathrm{DEG}}} + \frac{-\sigma(x)}{t_{2\mathrm{DEG}} + t_{\mathrm{AlGaN}}}} \right), \quad (2)$$

where t_{AlGaN} is the thickness of the barrier layer, t_{PZT} is the thickness of the PZT layer, $t_{2\mathrm{DEG}}$ is the distance between 2DEG and the polarization charge of the AlGaN surface. According to the C–V curve and the distribution of 2DEG, $t_{2\mathrm{DEG}}$ is taken as 1 nm. Equation (2) can be simplified as Eq. (3) after substituting the values of each thickness into the equation.

$$\sigma'(x) = \sigma(x) \cdot \left(1 + 0.0214 \times \frac{P_{\mathrm{PZT}}}{\sigma(x)} \right). \quad (3)$$

According to Eq. (3), it can be concluded that the polarization charge of PZT must be an order of magnitude larger than that of AlGaN in order to have a significant effect on the device performance. Capacitor of PZT and AlGaN are connected in series. The 2DEG concentration formula of MIS-HEMTs can be obtained from[17]

$$N_{\mathrm{S}}(x) = \frac{\sigma'(x)}{e} - \left(\frac{C_{\mathrm{AlGaN}}}{e} \right) [\phi_{\mathrm{B}}(x) + E_{\mathrm{F}}(x) + \Delta E_{\mathrm{C1}}(x) - \Delta E_{\mathrm{C2}}(x)] \frac{C_{\mathrm{PZT}}}{C_{\mathrm{PZT}} + C_{\mathrm{AlGaN}}}, \quad (4)$$

where $\phi_{\mathrm{B}}(x)$ is the Schottky-barrier height, E_{F} is the difference between Fermi level and GaN conduction band edge level, and ΔE_{C1} and ΔE_{C2} is the conduction band discontinuity between PZT and AlGaN, and AlGaN and GaN.

Figure 5(a) shows the trend of polarization charge and electron concentration. With the increase of PZT polarization charge, the equivalent polarization charge and the electron concentration increase linearly. When the polarization charge of PZT reaches 0.5 C/m^2, both of the equivalent polarization charge and the electron concentration increase by 48.6%. The polarization charge of PZT has a great ability to control the channel electron concentration. Figure 5(b) shows the trend of polarization charge of PZT with different gate voltages. According to the MFM structure in the reference,[11] the polarization charge of PZT has hysteresis in the process of gate voltage sweep back. The hysteresis characteristics of PZT are different with different sweeping speeds. When the speed of voltage scanning is faster, the hysteresis of the curve is larger because of the delay of the change of the planned charge. Therefore, in the process of voltage increasing, when the voltage sweeping speed is faster, the corresponding polarization charge is smaller.

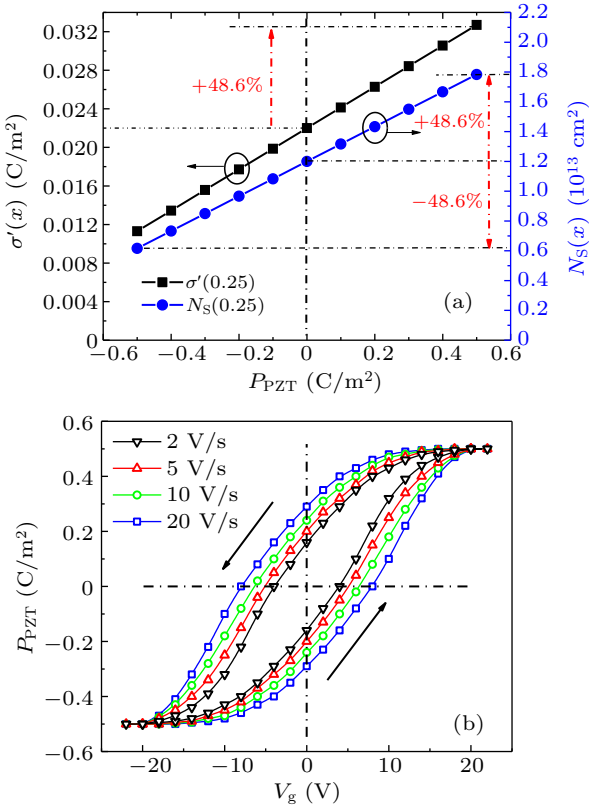


Fig. 5. (a) The trend of polarization charge and electron concentration and (b) the trend of polarization charge of PZT with different gate voltages.

For the HEMT devices, the current between source and drain (I_{DS}) can be calculated by

$$I_{\mathrm{DS}} = qWv(x)N_{\mathrm{S}}(x), \quad (5)$$

where W is the gate width, $v(x)$ is the velocity of the electrons in the channel. As the barrier layer is not etched, the

electron velocity is proportional to the electron mobility, and the electron mobility remains unchanged. The I_{DS} is mainly determined by the $N_S(x)$.

Capacitors of PZT and AlGaN are connected in series. Assuming that the 2DEG in the channel is totally depleted at V_{th}, the V_{th} can be expressed as[17]

$$V_{th} = \frac{1}{e}[\phi_B(x) + E_F(x) + \Delta E_{C1}(x) - \Delta E_{C2}(x)] - \sigma'(x)\left(\frac{t_{PZT}}{\varepsilon_0\varepsilon_{PZT}} + \frac{t_{AlGaN}}{\varepsilon_0\varepsilon_{AlGaN}}\right), \quad (6)$$

where ε_{PZT} is dielectric constant of PZT.

According to the above formula and experimental results, the experimental and theoretical results of I_{DS} and V_{th} can be obtained. Figure 6 shows that the theoretical values are in good agreement with the experimental results. The EPCM proposed in the present paper can guide the design of the PZT MIS-HEMT.

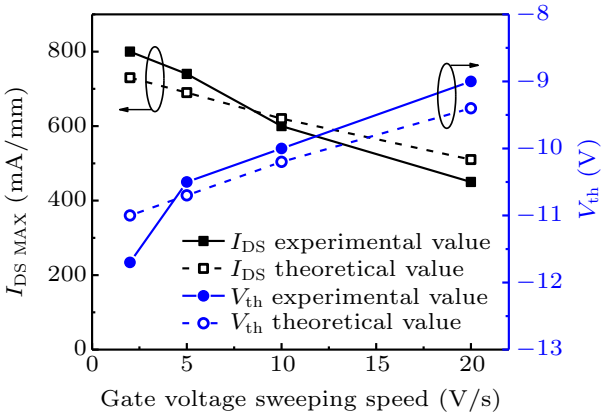


Fig. 6. Experimental and theoretical values of I_{DMAX} and V_{th} for the MIS-HEMT.

Figure 7 shows the change of the transfer characteristics with different gate voltage stresses. According to the results shown in Fig. 3, the transfer characteristics were tested with the sweeping speed of 2 V/s. The gate voltages were swept from −20 V to 10 V and the maximum gate voltage is equal to the stress voltage. This avoids the sweeping voltage having an influence on the stress effect. As shown in Fig. 7(a), the V_{th} increases from −11.2 V to −7.1 V after applying 10-V gate voltage for 210 s. The V_{th} has a positive shift with an increase time in the stress–gate voltage. Moreover, the V_{th} changes little from 150 s to 210 s, indicating that the modulation of polarization charge has reached the limit. The polarization of PZT in PZT/AlGaN/GaN HEMT is enhanced with an increase time and this means that more negative polarization charges of PZT are switched in the PZT/AlGaN interface. Therefore, the two-dimensional electron gas density at the channel decreases, and V_{th} has a positive shift. Figure 7(b) shows that the V_{th} decreases from −7 V to −11 V after applying −20-V gate voltage for 210 s. The same principle as mentioned above is due to more positive polarization charges of PZT being switched in the PZT/AlGaN interface.

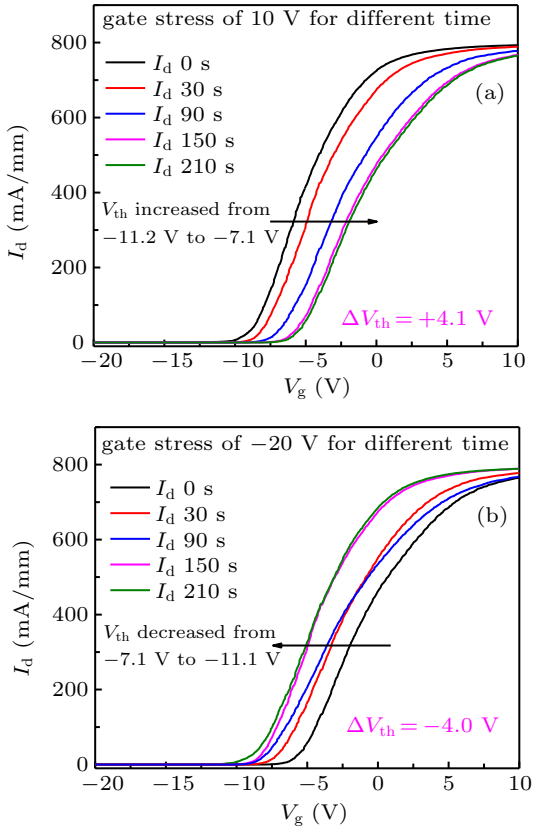


Fig. 7. (a) Transfer characteristics of 10-V gate stress for different time and (b) transfer characteristics of −20-V gate stress for different time.

Figure 8(a) shows the comparison of output characteristics before and after the gate-voltage stress. After a gate-voltage stress of 10 V for 120 s, the maximum output current density only decreased from 781 mA/mm to 779 mA/mm and the current density decreased from 518 mA/mm to 424 mA/mm when the gate voltage is 10 V and −2 V, respectively. After the stress is applied, the V_{th} is positively biased, which leads to the decrease of the output current at the same gate voltage. The on resistance (R_{on}) also remains unchanged before and after the stress, which is 4.6 Ω·mm. This shows that the gate voltage can modulate V_{th} of the device. When testing the output current curves, the drain voltage increases from 0 V to 10 V by keeping the gate voltage bias unchanged. Therefore, when the gate voltage is stable, the polarization charge is fixed and the output characteristics of the device remain stable.

Figure 8(b) shows a dual-pulse current collapse test performed on the device. In the test, the pulse width is 5×10^{-7} s, with 1-ms period and 1.5×10^{-7}-s rise time and the decline time.[18] The current collapse test selects two static operating points, the $(V_{gs}, V_{ds}) = (0, 0)$ state and the $(V_{gs}, V_{ds}) = (-8, 10)$ state. According to the measurement, the current collapse of the MIS-HEMT is 5.2%. Because the voltage change in the current collapse test is at the microsecond level and the change of polarization charge takes many seconds, the polarization charge has no time to follow the change of the gate voltage. Therefore, the current collapse of the device is very small and the current collapse characteristic is very stable.

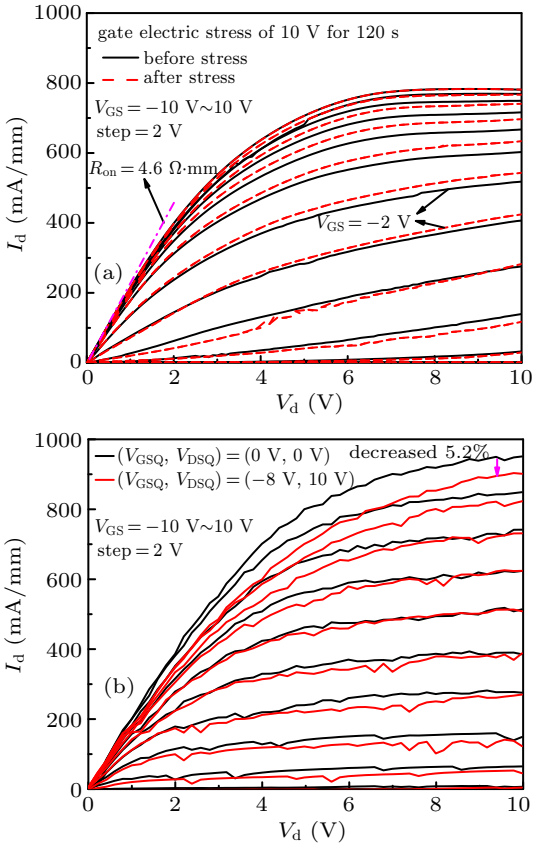


Fig. 8. (a) Output current curves of before and after gate stress for 120 s and (b) pulse output current curves of the devices.

The multi-frequency *C*–*V* characteristics are shown in Fig. 9. The *C*–*V* curves of different frequencies are basically coincident, and the maximum value of dispersion is only 0.3 V. At the same time, the *C*–*V* curves is swept back and the maximum hysteresis is 0.5 V. According to the results of the *C*–*V* curves, the V_{th} is stable when the polarization charge is fixed. In the *C*–*V* test, the frequencies are from 10 kHz to 1 MHz and the corresponding time is from 1 μs to 100 μs, respectively. The polarization charge is also difficult to keep up with the changing speed, so the polarization charge is also stable. Therefore, the V_{th} can be adjusted according to the modulation of polarization charge.

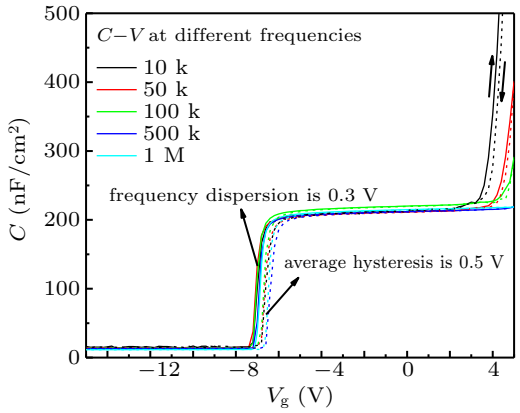


Fig. 9. Multifrequency *C*–*V* curves of PZT MIS-HEMT.

4. Conclusion

The $PbZr_{0.2}Ti_{0.8}O_3$ AlGaN/GaN metal–insulator–semiconductor high electron mobility transistors (MIS-HEMT) is fabricated on the sapphire substrate. The ferroelectric effect is shown in the transfer characteristics. The amount of polarization charges in PZT are different at different sweeping voltage speeds. An equivalent polarization charge model is proposed for calculating the concentration of 2DEG. The threshold voltage (V_{th}) and output current density (I_{DS}) can be obtained by the theoretical model. The theoretical values are in good agreement with the experimental results and the model proposed can guide the design of the PZT MIS-HEMT. The polarization charges of PZT can be modulated by different gate-voltage stresses. So the V_{th} have a regulation range of 4.0 V. The polarization charge changes after the stress of gate voltage for several seconds. When the gate voltage is stable or changes at high frequency, the output characteristics and the current collapse of the device remain stable.

References

[1] Chen C C, Hua M Y, Chen J T, Song Y, Zheng Z Y, Wei J and Chen K J 2020 *IEEE Electron Dev. Lett.* **41** 545
[2] Shi Y J, Chen W J, Sun R Z, Liu C, Xin Y J, Xia Y, Wang F Z, Xu X R, Deng X C, Chen T S and Zhang B 2020 *IEEE T. Electron. Dev.* **67** 2290
[3] Lee H P and Bayram C 2020 *IEEE T. Electron. Dev.* **67** 2760
[4] Hua M Y, Yang S, Wei J, Zheng Z Y, He J B and Chen K J 2020 *IEEE T. Electron. Dev.* **67** 217
[5] Asubar J T, Kawabata S, Tokuda H, Yamamoto A and Kuzuhara M 2020 *IEEE Electron Dev. Lett.* **41** 693
[6] Sun Z H, Huang H L, Wang R H, Sun N, Tao P C, Ren Y S, Sun S K, Wang H Z, Li S Q, Cheng W X, Gao J and Liang H N 2020 *IEEE Electron Dev. Lett.* **41** 135
[7] Erine C, Ma J, Santoruvo G and Matioli E 2020 *IEEE Electron Dev. Lett.* **41** 321
[8] Yu C J, Hsu C W, Wu M C, Wu W C, Chuang C Y and Liu J Z 2020 *IEEE Electron Dev. Lett.* **41** 673
[9] Lee C H, Yang C L, Tseng C Y, Chang J H and Horng R H 2015 *IEEE T. Electron Dev.* **62** 2481
[10] Tan A J, Chatterjee K, Zhou J R, Kwon D, Liao Y H, Cheema S, Hu C M and Salahuddin S 2020 *IEEE Electron Dev. Lett.* **41** 240
[11] Chen L X, Wang H, Hou B, Liu M, Shen L K, Lu X L, Ma X H and Hao Y 2019 *Appl. Phys. Lett.* **115** 193505
[12] Chen L X, Ma X H, Zhu J J, Hou B, Song F, Zhu Q, Zhang M, Yang L and Hao Y 2018 *IEEE T. Electron. Dev.* **65** 3149
[13] Wang H Y, Wang J Y, Li M J, Cao Q R, Yu M, He Y D and Wu W G 2018 *IEEE Electron Dev. Lett.* **39** 1888
[14] Hou B, Ma X H, Zhu J J, Yang L, Chen W W, Mi M H, Zhu Q, Chen L X, Zhang R, Zhang M, Zhou X W and Hao Y 2018 *IEEE Electron Dev. Lett.* **39** 397
[15] Zhu J J, Chen L X, Jiang J, Lu X L, Yang L, Hou B, Liao M, Zhou Y C, Ma X H and Hao Y 2018 *IEEE Electron Dev. Lett.* **39** 79
[16] Ambacher O, Smart J, Shealy J R, Weimann N G, Chu K, Murphy M, Schaff W J and Eastman L F 1999 *J. Appl. Phys.* **85** 3222
[17] Zhao Y P, Wang C, Zheng X F, Ma X H, He Y L, Liu K, Li A, Peng Y, Zhang C F and Hao Y 2020 *Solid State Electron.* **163** 107649
[18] Zhao Y P, Wang C, Zheng X F, Ma X H, Liu K, Li A, He Y L and Hao Y 2020 *Chin. Phys. B* **29** 087304